Mon. Not. R. Astron. Soc. **000**, 1–?? (2013) Printed 9 July 2015 (MN LATEX style file v2.2)

A millimeter-wave redshift search for the unlensed HyLIRG, HS1700.850.1

S. C. Chapman[1⋆], F. Bertoldi,[2] Ian Smail,[3] C. C. Steidel,[4] A. W. Blain,[5] J. E. Geach,[6] M. Gurwell,[7] R. J. Ivison,[8,9] G. R. Petitpas,[7] N. Reddy[10]

[1]*Department of Physics and Atmospheric Science, Dalhousie University, Halifax, NS, B3H 4R2, Canada*
[2] *Argelander-Institute of Astronomy, Bonn University, Auf dem Hugel 71, D-53121 Bonn, Germany*
[3]*Centre for Extragalactic Astronomy, Department of Physics, Durham University, South Road, Durham DH1 3LE*
[4]*Cahill Center for Astronomy and Astrophysics, California Institute of Technology, MS 249-17, Pasadena, CA 91125, USA*
[5]*Physics and Astronomy, University of Leicester, University Road Leicester, LE1 7RH*
[6]*Centre for Astrophysics Research , Science & Technology Research Institute, University of Hertfordshire, Hatfield AL10 9AB, UK*
[7]*Harvard-Smithsonian Center for Astrophysics, 60 Garden Street, Cambridge, MA 02138*
[8]*Institute for Astronomy, University of Edinburgh, Royal Observatory, Blackford Hill, Edinburgh, EH9 3HJ, UK*
[9]*European Southern Observatory, Karl Schwarzschild Strasse 2, D-85748 Garching, Germany*
[10]*Department of Physics and Astronomy, UC Riverside, 900 University Avenue, Riverside, CA 92521*

arXiv:1503.02195v2 [astro-ph.GA] 8 Jul 2015

Submitted for publication in MNRAS

ABSTRACT

We report the redshift of an unlensed, highly obscured submillimetre galaxy (SMG), HS1700.850.1, the brightest SMG ($S_{850\mu m}$=19.1 mJy) detected in the JCMT/SCUBA-2 Baryonic Structure Survey, based on the detection of its ^{12}CO line emission. Using the IRAM PdBI-WIDEX with 3.6 GHz band width, we serendipitously detect an emission line at 150.6 GHz. From a search over 14.5 GHz in the 3-mm and 2-mm atmospheric windows, we confirm the identification of this line as ^{12}CO(5–4) at $z = 2.816$, meaning that it does not reside in the $z \sim 2.30$ proto-cluster in this field. Measurement of the 870μm source size ($<0.85''$) from the Sub-Millimeter Array (SMA) confirms a compact emission in a $S_{870\mu m}$ =14.5 mJy, $L_{IR}\sim10^{13}\,L_{\odot}$ component, suggesting an Eddington-limited starburst. We use the double-peaked ^{12}CO line profile measurements along with the SMA size constraints to study the gas dynamics of a HyLIRG, estimating the gas and dynamical masses of HS1700.850.1. While HS1700.850.1 is one of the most extreme galaxies known in the Universe, we find that it occupies a relative void in the Lyman-Break Galaxy distribution in this field. Comparison with other extreme objects at similar epochs (HyLIRG Quasars), and cosmological simulations, suggests such an *anti-bias* of bright SMGs could be relatively common, with the brightest SMGs rarely occupying the most overdense regions at z =2–4.

Key words: galaxies: abundances – galaxies: high-redshift – submillimeter: galaxies.

1 INTRODUCTION

Blank-field mm and submm continuum surveys have discovered hundreds of dusty, star-forming submm galaxies (SMGs) over the past decade (e.g., Smail et al. 2002; Borys et al. 2003; Greve et al. 2004; Coppin et al. 2006; Bertoldi et al. 2007; Scott et al. 2008; Weiss et al. 2009), while *Herschel*-SPIRE has mapped close to 10^3 deg^2 in the 500, 350, 250μm bands, leading to $\sim10^4$ SMGs being detected (e.g., Oliver et al. 2010). At higher flux limits SPT has mapped 2500 deg^2 (e.g., Mocanu et al. 2013), and *Planck* has mapped the entire sky (Planck collaboration et al. 2014), finding many extreme and/or gravitationally lensed SMGs. The search for the most luminous star forming galaxies from 100's of deg^2 in the Universe has ensued (e.g,. Fu et al. 2013, Ivison et al. 2013). However some of the SMGs discovered in early $\sim$100 arcmin^2 surveys remain the intrinsically brightest, most extreme known (e.g., SMM J02399 – Ivison et al. 1998, 2010, GN20 – Pope et al. 2006; Younger et al. 2008, and COSMOS-AzTEC1 – Scott et al. 2008; Younger et al. 2010).

Determining the redshifts of unlensed SMGs has largely been a process of using weak counterparts in the rest-frame ultraviolet and optical to make spectroscopic determinations (e.g,. Chapman et al. 2003, 2005), or combining near- and mid-IR photometry to obtain reliable photometric redshift estimates (e.g., Wardlow et al. 2011; Simpson et al. 2014). However, because the high extinction of SMGs means that they often have only very faint (if any) counterparts in the optical/near-IR bands, the spectroscopic and even

⋆ scott.chapman@dal.ca

© 2013 RAS

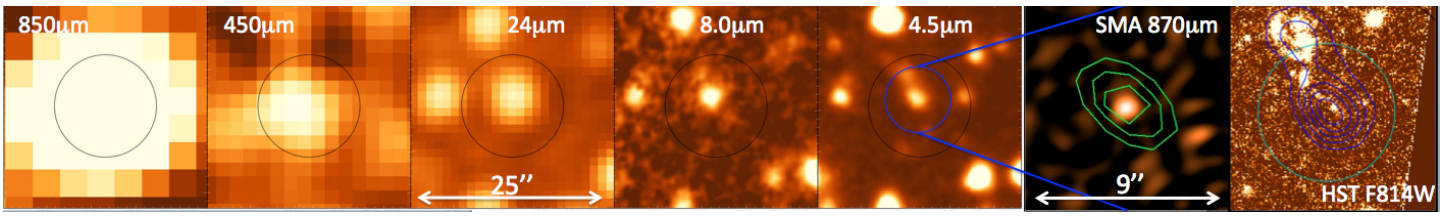


Figure 1. Left to right: Five cutout images 25″ on a side of the longer wavelength data for HS1700.850.1 (850μm, 450μm, 24μm, 8μm, 4.5μm), highlighting the likely identification of the SMG with an IR-luminous component (black circle shows the 15″ SCUBA-2 beam size). **Second from right:** A 9″×9″ zoom in from the SMA compact+extended configuration 870μm map, with a $\sim$ 0.74″ synthesized beam with PdBI ^{12}CO(5–4) contours overlaid. Most of the SCUBA-2 flux (14.5 mJy) is recovered in a single compact component, unresolved with a 1″ beamsize. No other significant sources are detected within the 15″ diameter of the SCUBA-2 beam. Further, the compact configuration data on its own measures a flux of 19±3 mJy, comparable to the SCUBA-2 flux, and suggestive that the source may be marginally resolved on scales $>$ 1″. **Far right:** 9″ cutout of the *HST*-ACS F814W image centred on the SMA detection, with IRAC ch-2 contours overlaid, shows HS1700.850.1 to be well identified with a faint tad-pole like $I_{AB} \sim 26$ galaxy, which is marginally detected in ground based imaging ($\mathcal{R} = 26.1$).

photometric redshift distributions have remained incomplete and biased (e.g., Simpson et al. 2014).

The largest spectroscopic SMG redshift survey to date was based on radio-identified SMGs (Chapman et al. 2005). The radio identification is sometimes inaccurate (Hodge et al. 2013) and may bias the redshift distribution since radio emission may remain undetected even in the deepest radio maps for sources at $z > 3$. Optical spectroscopic followup to ALMA-identified SMGs (Simpson et al. 2014; A. Danielson et al. in prep) have removed the identification bias, yet cannot remove the spectroscopic bias.

An alternative route to determine the redshift of an SMG is through observations of ^{12}CO emission lines at cm or mm wavelengths. The ^{12}CO lines arise from the molecular gas, the fuel for star formation, and can thus be related unambiguously to the submm continuum source. Therefore, these observations do not require any additional multi-wavelength identification and circumvent many of the problems inherent to optical spectroscopy of SMGs. However, to date the sensitivity of mm-wave facilities has limited the approach to followup of bright, gravitationally lensed SMGs (e.g., Weiss et al. 2009; Swinbank et al. 2010; Harris et al. 2012; Vieira et al. 2013; Zavala et al. 2015).

While the IRAM Plateau de Bure Interferometer (PdBI) is sensitive enough to detect ^{12}CO in unlensed SMGs (e.g. Bothwell et al. 2013), its 3.6 GHz bandwidth receivers limit this approach due to the large time requirement for blind searches of ^{12}CO lines in redshift space via multiple frequency tunings. Walter et al. (2012) observed the HDF-N field with the PdBI over the full 3mm window to a similar depth as the Bothwell et al. (2013) survey, requiring 110 hrs on-source. In addition to blindly detecting two faint ^{12}CO emitting galaxies, they identified the redshift of the $S_{850\mu m}$ $\sim$5 mJy HDF850.1 as $z = 5.3$. The 8-GHz instantaneous, dual-polarization bandwidth of ALMA, coupled with its sensitivity, improves this approach, but still makes it a relatively expensive prospect to blindly obtain ^{12}CO redshifts for even the brightest SMGs with $S_{850\mu m}$ $\sim$8 mJy.

In this paper, we describe a photometric redshift guided, mm-wave search for ^{12}CO line emission from HS1700.850.1, one of the brightest unlensed SMGs ever discovered, with $S_{850\mu m} = 19.1$ mJy. The target field was chosen from the 24 survey fields of the Keck Baryonic Structure Survey (KBSS – e.g., Rudie et al. 2012). Several of these fields show strong galaxy overdensities (e.g., Steidel et al. 2000, 2005, 2010), and together represent a complete, unbiased census of overdensities in a well-calibrated field galaxy survey at $z > 2$. The HS1700+64 field in which HS1700.850.1 was found hosts a well characterized $z = 2.30$ protocluster, studied in detail in several works (Steidel et al. 2005; Shapley et al. 2005; Digby-North et al. 2010). The faintness of HS1700.850.1 at near-IR/optical wavelengths precluded spectroscopic observations, despite lying in this well studied field.

We use cosmological parameters Ω_m = 0.3, Λ = 0.7, and H = 70 km s^{-1} Mpc^{-1} throughout the paper; at $z = 2.82$, this corresponds to an angular scale of 7.94 kpc arcsec^{-1}, or 0.48 Mpc arcmin^{-1}.

2 OBSERVATIONS AND STRATEGY

The HS1700+64 field was targeted with SCUBA-2 at the JCMT as part of a submm-wave followup of six KBSS fields (K. Lacaille et al. in prep), covering $\sim$ 0.19 deg^2. The brightest source in this 850μm survey is HS1700.850.1 with $S_{850\mu m}$=19.1±0.8 mJy. Fig. 1 shows cutouts of HS1700.850.1 at SCUBA-2 and *Spitzer* wavelengths, revealing a likely identification at 4.5μm.

The HS1700+64 field contains a massive proto-cluster at $z = 2.30$ (Steidel et al. 2005), and given its 1.5′ proximity to the cluster centre, HS1700.850.1 was considered a likely cluster member. HS1700.850.1 has two candidate *Spitzer*-IRAC identifications within 4″ of the 850μm centroid, one of which is associated with a well detected complex of $z = 2.305$ galaxies. IRAM-PdBI observations targeting ^{12}CO(3–2) and [CI] at $z = 2.305$ in the 3mm and 2mm bands respectively showed no detectable line emission, indicating this redshift was incorrect (Fig. 2). However, the WIDEX receiver's 3.6 GHz wide spectrum revealed a strong line detected serendipitously at 150.6 GHz near the edge of the chosen 2mm-band setting (Figs. 2,3). Two followup observations targeted the three most likely redshifts, assuming this 150.6 GHz line was a ^{12}CO rotational transition, as described in § 3.1. We also draw on *Spitzer*-IRAC, ground-based and *HST* optical datasets described by Steidel et al. (2011). All flux measurements are shown in Fig. 4, and discussed in § 3.1.

2.1 JCMT/SCUBA-2 Observations

SCUBA-2 observations were conducted in Band 2 weather conditions ($\tau_{225\rm GHz} < 0.08$) over 6 nights between 23rd May and 15th Oct. 2013, totalling 15 hours of on-sky integration in individual 30 min scans. A standard 3′ diameter "daisy" mapping pattern was used, which keeps the pointing centre on one of the four SCUBA-2 sub-arrays at all times during exposure. Data reduction followed standard recipes (e.g., Geach et al. 2013), with individual

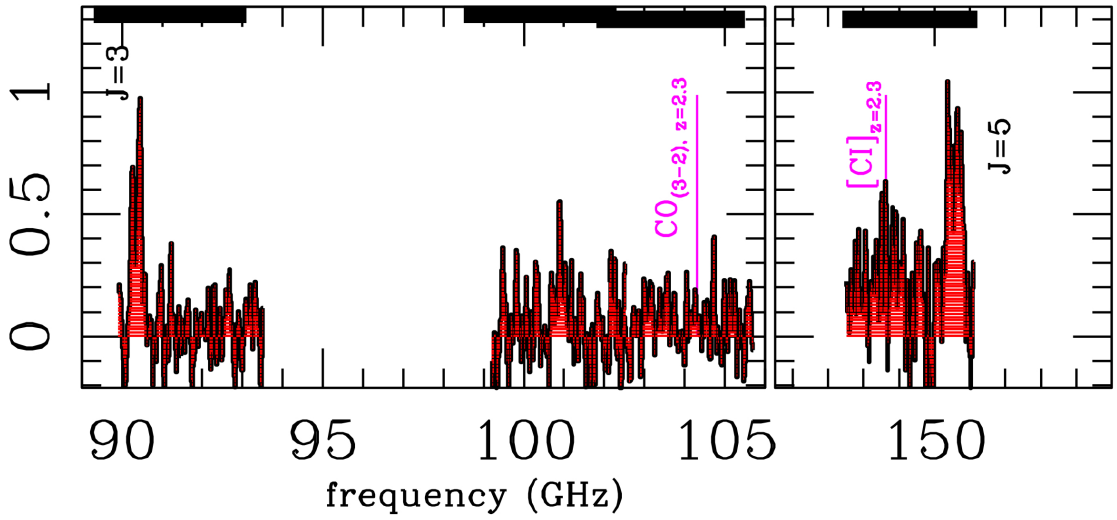


Figure 2. A composite of all spectral scans towards HS1700.850.1, shown at a velocity resolution of 60 km s^{-1} (arbitrary flux scaling). ^{12}CO emission lines are seen at $\sim$ 90.2 and 150.6 GHz, the latter corresponding to ^{12}CO(5–4). The originally targeted $z = 2.31$ ^{12}CO and [CI] line frequencies are highlighted (magenta), with a curious excess seen at the [CI] frequency. The four tuning bands are marked with heavy lines, showing a slight overlap near 101 GHz.

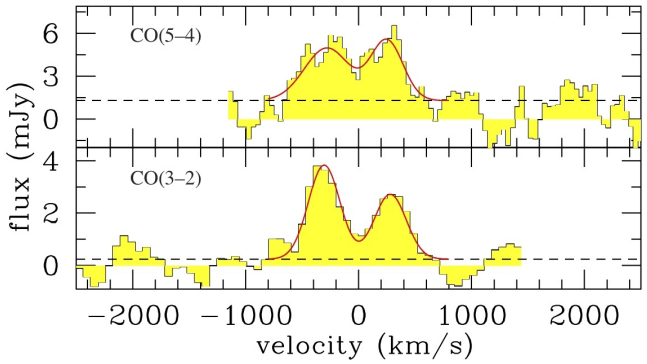


Figure 3. Spectra of the ^{12}CO(3–2) and ^{12}CO(5–4) lines towards HS1700.850.1. The spectral resolution is 60 km s^{-1} for both lines. We find only marginal evidence for any spatial separation in the two peaks of the CO lines $< 1''$. Double Gaussian fits to each line profile are overlaid, emphasizing the $\sim$50% higher peak flux in the blue component of the CO(3–2) profile. Line ratio and dynamical modelling issues are discussed in detail in the text.

Table 1. PdBI observations log.

Run-ID	center freq (GHz)	$t^a_{\rm int}$ (hr)	Depth^b (mJy)	obs date	beamsize
S14ck001	103.8	3.34	0.60	09/06/14	$5.1''\times4.2''$
S14ck002	149.2	3.45	1.12	11/06/14	$3.5''\times2.7''$
D14d001	100.8	1.50	0.95	28/07/14	$4.7''\times4.0''$
D14d002	91.7	3.15	0.43	04/08/14	$4.8''\times4.1''$

[a] 5-Antenna integration.

[b] per 50MHz channel.

30 min scans reduced using the dynamic iterative map-maker of the SMURF package (Jenness et al. 2011), flat-fielding, and then solving for model components assumed to make up the bolometer signals (atmospheric, astronomical, and noise terms). The signal from each bolometer's time stream is then re-gridded onto a map, with the contribution to a given pixel weighted according to its time-domain variance. Filtering of the time-series is performed in the frequency domain, with band-pass filters equivalent to angular scales of $2'' < \theta < 120''$, along with 10σ deviation *spike* removal in a moving boxcar, and DC step corrections. Finally, since we are interested in (generally faint) extragalactic point sources, we apply a beam matched filter to improve point source detectability, resulting in a map that is convolved with an estimate of the 850μm beam. The map reaches central noise levels of σ_{850}=0.51 mJy and σ_{450}=6.4 mJy.

Table 2. Photometry of HS1700.850.1

Band	Flux	Instrument
91.7GHz	0.25±0.07 (mJy)	PdBI
100.8GHz	0.31±0.13 (mJy)	PdBI
103.8GHz	0.38±0.08 (mJy)	PdBI
149.2GHz	1.39±0.15 (mJy)	PdBI
850μm	19.1±0.8 (mJy)	SCUBA-2
870μm	14.5±1.1 (mJy)	SMA
450μm	45±6 (mJy)	SCUBA-2
24μm	171±7 (μJy)	MIPS
8.0μm	13.2±1.2 (μJy)	IRAC
4.5μm IRAC	10.2±0.9 (μJy)	IRAC
K_s(2.18μm)	23.20±0.13 (AB mag)	P200/WIRC
J(1.25μm)	24.4±0.2 (AB mag)	P200/WIRC
I(F814W)	25.8±0.2 (AB mag)	HST/ACS
$\mathcal{R}$ [a]	26.1±0.3 (AB mag)	WHT/PFC
g'	27.0±0.3 (AB mag)	WHT/PFC
u'	>27.1, 3σ (AB mag)	WHT/PFC

[a] The $\mathcal{R}$ filter is centered at 6900Å and thus redder than the standard R – close to mid-way between SDSS r' and i' in effective wavelength

2.2 IRAM/PdBI Observations

The IRAM-PdBI observations were taken in D configuration using the 5-antenna sub-array (properties of the observing runs and resulting synthesized beam sizes are summarized in Table 1), at a

pointing center: RA=17 01 17.779, Dec=+64 14 37.85, J2000.0, taken from the SCUBA-2 centroid. Flux calibration was achieved by observing various calibrators (3C273, 3C345, B0234+285, B1749+096). The quasar B1300+580 was used as a phase and amplitude calibrator. Data were processed using the most recent version of the GILDAS software. We resampled the cubes in 90 km s^{-1} channels, and imaged them using the GILDAS suite *mapping*, adopting natural weighting. The full PdBI spectrum is shown in Fig. 2. To obtain flux measurements, we deconvolved the visibilities using the CLEAN task with natural weighting, and applied the corresponding primary beam correction (negligible at the small 3″ offset of the HS1700.850.1 position).

2.3 SMA observations

Followup SMA observations were performed on August 15 and September 7, 2014 in the compact and extended configurations respectively (beam sizes ∼2″ and ∼0.85″ respectively) in good weather ($\tau_{225\rm GHz} \sim 0.08$) with a total on-source integration time of approximately 6 hr. The USB was tuned to 345 GHz, and combined with the LSB for an effective bandwidth of ~ 4 GHz at 340 GHz, which yielded a final rms of 1.1 mJy. The pointing centre was the same as that for the PdBI observations described above. The data were calibrated using the MIR software package (Scoville 1993), modified for the SMA. Passband calibration was done using 3C 84, 3C 111, and Callisto. The absolute flux scale was set using observations of Callisto and is estimated to be accurate to better than 20%. Time-dependent complex gain calibration was done using 1858+655 (0.6 Jy, 21.8° away) and 1827+390 (1.8 Jy, 37.7° away). We detect HS1700.850.1 in the synthesized image at $\sim 13\sigma$. The calibrated visibilities were best fit by a single point source with an integrated flux density of $S_{890\mu\rm m} = 14.5 \pm 1.1$ mJy at a position of α(J2000) =17 01 17.779 and δ(J2000) = +64 14 37.85, consistent within 0.3″ with the centroid of the line and continuum measurements from PdBI. The astrometric uncertainties are $\Delta\alpha = 0.24$ arcsec (0.20 arcsec systematic; 0.13 arcsec statistical) and $\Delta\delta = 0.22$ arcsec (0.19 arcsec systematic; 0.10 arcsec statistical).

3 RESULTS

3.1 The redshift search

Our original IRAM-PdBI observations searched for the ^{12}CO and [CI] lines in HS1700.850.1 at a redshift ~ 2.30. This was motivated by it lying near the core of a massive $z = 2.31$ protocluster in the Keck Baryonic Structure Survey (Steidel et al. 2011), and having a plausible 4.5μm identification with a complex of known $z = 2.305$ BX galaxies. Being such an extreme source we would not expect to find it by chance in the small 0.03 deg^2 H1700+64 pointing, or even in the 0.19 deg^2 survey of the six KBSS fields without the high density environment of the proto-cluster in this field. Using typical single dish 850μm counts (Coppin et al. 2006; Weiss et al. 2009) we expect a surface density of just 0.01 deg^{-2} for such 19 mJy sources. The source counts of the brightest submm sources (S870μm>9 mJy) measured by ALMA fall more steeply than those measured with lower resolution single-dish observations due to the multiplicity of the brightest sources when observed at arcsecond resolutions (e.g., Karim et al. 2013). As HS1700.850.1 retains at least ∼15 mJy in the interferometric followup (and as much as 19 mJy if the compact configuration SMA data is taken at face value), the expected >15 mJy source density drops by another factor of ten based on the ALMA-derived count of Karim et al. (2013) or Simpson et al. (2015b).

The IRAM-PdBI observations showed no such lines at the expected frequencies, and thereby implied that the proposed identification and redshift of $z \sim 2.31$ was incorrect. As the 7.2 GHz of frequency coverage did reveal a strong line detected serendipitously at 150.6 GHz near the edge of the 2mm setting, we began a search to identify the correct redshift. The centroid of this 150.6 GHz line detection, as well as the PdBI 2mm and 3mm continuum detections of HS1700.850.1, both localize the emission from the source within optical/IR imagery to within $\sim 0.5''$ (Fig. 1), while followup SMA 870μm continuum imaging unequivocally associates the 850μm SCUBA-2 source to a single IRAC galaxy which is well detected in the *HST* F814W image (Fig. 1) revealing a faint disturbed, tadpole-like galaxy. Ground-based imagery marginally detects the galaxy at $\mathcal{R} = 26.1$, $g = 27$, $U > 27.1$, making optical spectroscopy very difficult, and the $z = 2.82$ redshift would be difficult for near-IR spectroscopy, although the $K_{s,AB} = 23.2$ is feasible in general with a 10m telescope. Note that these colors (e.g., $g' - \mathcal{R}$ = 0.9 mag) make sense for a heavily reddened object at z=2.82. However, the detection at g'-band, places loose constraints on the redshift to $z < 4$, while the comparable IRAC fluxes, S(4.5μm)=10.2μJy .and S(8.0μm)=13.2μJy suggests the 1.6μm stellar bump should lie between, ranging between 2.4<z<3.7. The very red $K_s - 4.5\mu$m coloyr (1.8 mags AB) is large, though consistent with a high stellar mass object. The MIPS 24μm flux of 0.17 mJy compared to the $S_{850\mu\rm m}$ flux suggests that PAH emission is not contributing to the 24μm band, pushing the redshift to $z > 2.5$, as illustrated in the SED template fit (Fig. 4). Our final constraint on the redshift comes from the long-wavelength photometry (Fig. 4, Table 2), where 3mm, 2mm, 870μm, and 450μm fluxes suggest a similar range of 2.5<z<4.5 for a likely range of SMG dust temperatures, 25 K<$T_{\rm d}$<45 K.

While these constraints may not seem very useful, the fact that we have a solid line detection at 150.6 GHz means that only three possible ^{12}CO identifications provide redshifts in this range: ^{12}CO(4–3) at $z = 2.82$, ^{12}CO(5–4) at $z = 3.58$, or ^{12}CO(6–5) at $z = 4.37$. Aided by these photometric redshift estimates, in two subsequent PdBI followup observations we searched for $z = 3.58$ ^{12}CO(4–3) at 100.4 GHz, and then at 91.5 GHz searched simultaneously for $z = 2.82$ ^{12}CO(4–3) and [CI] at $z = 4.37$. With a detection of a second line (Fig. 2) we confirmed the redshift z=2.816 for one of the most intrinsically luminous galaxies in the distant Universe ($L_{\rm FIR} \sim 5 \times 10^{13} L_\odot$, § 3.3) and secured a second ^{12}CO line for astrophysical diagnostics. Blind ^{12}CO redshifts for unlensed SMGs are still exceedingly rare in the literature. We are only aware of Daddi et al. (2009) GN20 at $z = 4.05$ (a truly serendipitous discovery), and the $z = 5.2$ for HDF850.1 (Walter et al. 2012).

3.2 Source properties

HS1700.850.1 is very bright at 850μm, but shows no sign of lensing – the nearest galaxy detected is the low-mass star forming galaxy BX951 2.9″ away (z=2.3053, $M^* = 2 \times 10^9$ M$_\odot$). HS1700.850.1 is thus not suffering from differential lensing and associated modelling issues and biases that could affect our interpretation of the ^{12}CO lines. The ^{12}CO spectra are shown zoomed in at a velocity resolution of 60 km s^{-1} in Fig. 3. Both lines are detected at high significance (11.3 σ and 6.9 σ for continuum subtracted (3–2) and (5–4) lines respectively, in integrated intensity). The line

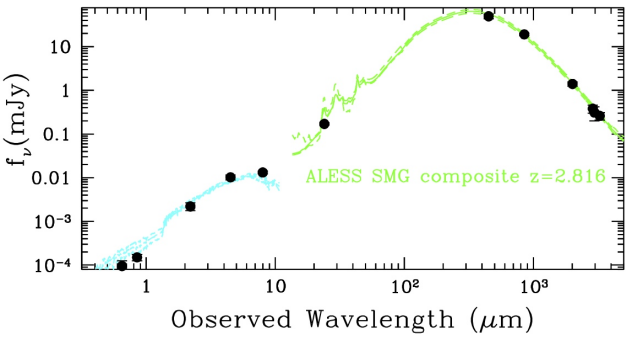


Figure 4. The SED of HS1700.850.1, with the Swinbank et al. (2014) composite SMG template overlaid. Significantly hotter or cooler SEDs than this $\sim 35K$ template are reasonably rejected by the photometry. The template is split at a rest frame 10μm in order to fit the optical/near-IR faint component as decoupled from the luminous far-IR to submm dust component. The far-IR luminosity of this model is $3.8 \cdot 10^{13}\ L_\odot$.

Table 3. Gaussian decomposition of the CO line spectra. Values for the total line are estimated from integrating the continuum-subtracted spectra, while the red and blue component properties are estimated from the Gaussian fits. Errors in redshift estimation are dz=0.001. The measured FWHM for the total line is quoted as σ, 2.355× smaller. $L'CO$ is in units of 10^{10} K km s^{-1} pc^2. Note that for α(CO)=1 M$_\odot$ (K km s^{-1} pc^2)$^{-1}$, as estimated in Bothwell et al. (2013), $L'CO_{1-0}$ = M(gas), which should then be corrected by an additional 15% for Helium.

	blue	red	total
$z_{(3-2)}$	2.812	2.820	2.816
δv(3-2) [km s^{-1}][a]	-305 ± 9	$+280 \pm 11$	0
δv(5-4) [km s^{-1}][a]	-280 ± 21	$+250 \pm 19$	0
σ(3-2) [km s^{-1}]	140 ± 25	142 ± 20	400 ± 57[c]
σ(5-4) [km s^{-1}]	200 ± 45	143 ± 24	349 ± 45[c]
I_{3-2} [Jy km s^{-1}]	1.26 ± 0.16	0.88 ± 0.13	2.32 ± 0.21
I_{5-4} [Jy km s^{-1}]	1.84 ± 0.23	1.5 ± 0.21	3.44 ± 0.30
$L'CO_{3-2}$	5.18	3.62	9.65
$L'CO_{5-4}$	2.72	2.21	5.08
$L'CO_{1-0}$ [b]	9.95	6.95	18.56

[a] Center velocity relative to z=2.816.

[b] Derived using average r$_{31}$ = 0.32 scaling relation of Bothwell et al. (2013).

[c] These are the best fit single Gaussian to the entire line profile.

profiles for both lines are similar and well described by a double Gaussian with a peak separations of 585 and 530 km s^{-1}for (3–2) and (5–4) ^{12}CO lines respectively, and individual peak FWHMs of ∼330-470 km s^{-1}. While the (3–2) line shows an apparent peak flux asymmetry compared with the (5–4) peaks, in fact the flux ratios of the blue and red lines are quite similar, r$_{53,blue}$=0.69±0.12 and r$_{53,red}$=0.59±0.09. The parameters derived from Gaussian fits to both line profiles are given in Table 3. We find only marginal evidence for any spatial separation in the two peaks of either of the ^{12}CO lines $< 1''$. The frequencies unambiguously identify the lines as CO(3–2) and CO(5–4). Combining the centroids of both lines, we derive a variance-weighted mean redshift for HS1700.850.1 of $z = 2.816 \pm 0.001$. While the observed frequencies might also be interpreted as ^{12}CO(6–5) and ^{12}CO(10–9) at $z = 6.64$, the ^{12}CO ladder is not equidistant in frequency which results in small differences for the frequency separation of the line-pairs as a function of rotational quantum number. The frequency separation is 58.58 and 58.53 GHz for the ^{12}CO line-pairs at redshifts 2.82 and 6.64 respectively. Our observations yield $\delta\nu = 58.58 \pm 0.02$ GHz, clearly consistent with the former, and supported by the photometric redshift.

With the precise redshift and the observed ^{12}CO line luminosities in hand, we can estimate the molecular gas content of HS1700.850.1. The observed global ^{12}CO(5–4) to ^{12}CO(3–2) line ratio (0.67±0.09) implies that the CO emission is sub-thermally excited, at least for the CO(5–4) line. The average line ratio reported by Bothwell et al. (2013) for a sub-sample of their 30 SMGs is r$_{53}$=0.62. This line ratio is similar to that observed for SMM J16359+6612 (Weiss et al. 2005) and we use a similar scaling to estimate a ^{12}CO(1–0) line luminosity of $L' \approx 1.86 \cdot 10^{11}$ K km s^{-1} pc^2. This translates into a molecular gas mass of $M_{\rm H_2} \approx 2.1 \cdot 10^{11}$ M$_\odot$ using a standard ULIRG conversion factor of 1.0 M$_\odot$ (K km s^{-1} pc^2)$^{-1}$ found for typical $z \sim 2.5$ SMGs in Bothwell et al. (2013), and including a 15% contribution from Helium. (Downes et al. 1998 adopted 0.8 M$_\odot$ (K km s^{-1} pc^2)$^{-1}$).

3.3 SED modelling

The SED of HS1700.850.1, with the Swinbank et al. (2014) composite SMG template overlaid is shown in Fig. 4. Significantly hotter or cooler SEDs than this $\sim 35K$ template are reasonably rejected by the photometry. The template is split at a rest frame 10μm in order to fit the optical/near-IR faint component as decoupled from the luminous far-IR to submm dust component. The far-IR luminosity of this model is $3.8 \times 10^{13}\ L_\odot$, translating to a SFR of 2500 M$_\odot$ yr^{-1} (Kennicutt 1983). HS1700.850.1 is not unusually faint in optical/IR magnitudes for SMGs with S$_{850\mu m}$∼3-5 mJy, but its far-IR output is significantly higher, and it is thus proportionally far more obscured than ALESS SMGs (see Swinbank et al. 2014).

A hyper-z fit to the IRAC and near-IR photometry yields a stellar mass of 3×10^{11} M$_\odot$, assuming a Chabrier IMF. Together with the above gas mass estimate, the gas fraction is ∼40%, and precludes using substantially higher conversion factors, α(CO)$\gg$ 1, which would drive the gas fraction up towards 100%.

3.4 SMA and PdBI continuum maps and source multiplicity

The PdBI observations reveal only a single significant detection in both continuum and line emission, showing that there is no obvious multiplicity at 2mm/3mm or in CO lines. As such there are no nearby ($< 25''$ primary beam) ^{12}CO-luminous companions to HS1700.850.1. Similarly the SMA image does not detect any additional significant sources. The combined 3mm continuum map reaches 0.35 mJy rms. At this depth we are sensitive to SMGs with SFRs∼1000 M$_\odot$ yr^{-1}. The 2mm continuum map reaches 1.2 mJy rms and should detect similar SFRs for a typical $\beta \sim 1.5$ dust SED. The SMA 870μm map rms of 1.1 mJy is much more sensitive to dusty sources, and should detect galaxies with SFRs∼300 M$_\odot$ yr^{-1}. We note that a CO-luminous DRG in this field with a SFRs∼200 M$_\odot$ yr^{-1} from Chapman et al. (2015) is not detected in any of these continuum maps, nor are any of the other known galaxies lying within the primary beam.

By considering only the SMA compact configuration data ($2''$ beam size), we measure a larger flux density of 19.3±2.8 mJy, close to that measured by SCUBA-2 in the $14.5''$ beam, although the large measurement error agrees with the extended configuration flux measurement within $\sim 2\sigma$. Nonetheless, this may suggest there

is either a modest conflict in the flux scale between compact and extended configurations, or that the source may be marginally resolved on scales greater than the average beam size achieved in our extended configuration data, $> 0.85''$. However, this is unusual for bright SMGs (Simpson et al. 2015a) which typically are resolved with $\sim 0.3-0.4$ source sizes. Ubiquitous SMG multiplicity results from surveys (e.g., Wang et al. 2010, Hodge et al. 2013, Simpson et al. 2015b) and theoretical arguments (e.g. Hayward et al. 2012, 2013a, 2013b) would argue that there may well be faint companions within the SCUBA-2 beam, and the similarity of the compact SMA data flux may just be a lucky coincidence.

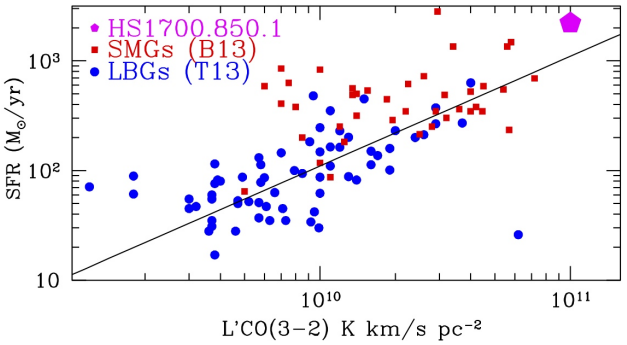


Figure 5. SFR versus L′CO(3-2) for various literature galaxies compared with HS1700.850.1 (normal star forming galaxies – Tacconi et al. 2013; SMGs – Bothwell et al. 2013). CO(3-2) is adopted for maintaining all displayed galaxies as close to observed transitions as possible. We show L′(CO) for HS1700.850.1, revealing it is nominally under-luminous in ^{12}CO compared to other ultra-luminous *normal* star forming galaxies, but not unusual compared to many SMGs in Bothwell et al. (2013) in lying a factor 2-3× above the Tacconi et al. (2013) best fit relation.

4 DISCUSSION

4.1 Gas dynamics

At first glance the double peaked line profile suggests a circumnuclear molecular toroid. However, if such a stable molecular gas distribution would supply the large star formation rate ($\approx 2500\,M_\odot\,yr^{-1}$), we would expect a high gas excitation. The observed line ratio r_{53}=0.67±0.09 is low compared to well-studied nearby starburst galaxies NGC 253 and M 82, although it is typical of that measured by Bothwell et al. (2013), a brightness temperature ratio r_{53}=0.62, for SMGs with characteristic $L_{850\mu m}$ lower than HS1700.850.1 by a factors of 3× on average. However, the two line peaks could also be two disk components merging, individually unresolved. The line integrated gas properties between the spectral components are similar in the red and blue component line ratios ($r_{53,red}$=0.6±0.1, $r_{53,blue}$=0.7±0.2), contrasting the component line widths and central velocities which do differ between the different excitation lines. This argues that the (5–4) line may be coming from a different volume of gas than the (3–2) line, which could be true in either a disk-like or merger configuration. If the SMA dust continuum size is the same as the CO gas ($< 0.85''$ or < 6.7 kpc), then either the disk or the merger is in a very compact state. We note that a ring-like rotating disk distribution of gas was strongly endorsed as an explanation for another similar double-peaked SMG, SMM J02399-0136 (Genzel et al. 2003), however from multi-frequency, high-resolution line mapping observations, Ivison et al. (2010) showed that the system comprises a multiple merger.

HS1700.850.1 is clearly a very massive system, and is in particular a very massive *baryonic* system. Observational studies of local ellipticals (Keeton 2001; Boriello, Salucci, & Danese 2003; cf. Loewenstein & Mushotzky 2003) suggest that typically $\sim 30\%$ of the total mass within the optical effective radius will be dark; the interior regions of massive local disk galaxies have similarly low dark matter fractions (Combes 2002). By analogy with these local systems, HS1700.850.1 should have a baryonic mass of $\geqslant 4\times10^{11}\,\sin^{-2} i^{-1}\,M_\odot$ within 7 kpc; $M_{gas} \sim 2\times10^{11}\,M_\odot$ then implies that a limit to the stellar mass within the same radius is $\sim 2\times10^{11}\,M_\odot$. The Kennicutt (1983) stellar initial mass function (IMF) models of Cole et al. (2001) imply that $M^* \sim 7\times10^{10}\,M_\odot$ for the galaxy stellar mass function in the local Universe. Based on the stellar content of its inner 7 kpc, then, HS1700.850.1 is already at least a $3M^*$ system, on its way to becoming a $\geqslant 4M^*$ system as it turns the remainder of its molecular gas into stars.

4.2 An Eddington-limited starburst?

If we assume that HS1700.850.1 is starburst dominated and make assumptions about the morphology and kinematics, we find it may be radiating close to or at the Eddington limit of its starburst. Elmegreen et al. (1999) demonstrated that feedback from ongoing star formation sets a physical limit on the minimum size of a star forming region. Radiation pressure from high luminosity star formation regions should produce strong momentum–driven winds due to high dust opacity seen by the ultraviolet light produced by young stars (e.g., Netzer & Elitzur 1993). These winds are confined by the gravitational potential, which scales as $\Phi \sim f_g\sigma^2 \log D$ for an isothermal sphere (with the gas fraction f_g, stellar velocity dispersion σ, diameter of the starburst region D). In the optically thin limit (appropriate for optically thick clouds with a small volume filling factor embedded in the diffuse interstellar medium) and assuming a Chabrier et al. (2003) initial mass function (IMF) this leads to a maximum star formation rate

$$\mathrm{SFR_{max}} = 360\,\sigma_{400}^2 D_{\rm kpc}\kappa_{100}^{-1}\ M_\odot\ yr^{-1} \quad (1)$$

We measure the scale size of the starburst $D_{\rm kpc}$ as the Gaussian FWHM of the SMA detected source, and σ_{400} as the line–of–sight ^{12}CO gas velocity dispersion in units of 400 km s^{-1} which is the best fit single Gaussian to the entire CO(3–2) line ; κ_{100} is the dust opacity in units of 100 cm^2 g^{-1}, which we set to 1, but note that many dust models allow for significantly higher opacity, and in particular for the ultraviolet radiation produced by young massive stars during a starburst (e.g., Li et al. 2001). HS1700.850.1 has a very high far-IR luminosity, with $L_{FIR} \approx 4\times10^{13}\ L_\odot$ and SFR $\approx 2500\ M_\odot\ yr^{-1}$ on a physical scale of < 7 kpc. This very luminous SMG is therefore near the Eddington limit $\leqslant 2000\ M_\odot\ yr^{-1}$ for a starburst on those scales. The size/SFR ratio of HS1700.850.1 is typical of the more luminous SMG components identified with ALMA observations by Simpson et al. (2015a), suggesting near Eddington-limited starbursts are not unusual in the SMG population. This motivates obtaining additional higher resolution 870μm and ^{12}CO observations of HS1700.850.1 to truly resolve the emission of this bright galaxy.

4.3 L'_{CO} to L_{FIR} comparison with literature

We next turn to a discussion of HS1700.850.1 versus other ^{12}CO-detected sources, plotting L'_{CO}-SFR for the known and published high-z sources (Fig. 5), and translating L_{FIR} to SFR in the SMG populations using standard conversions (Kennicutt 1983). Of note is that HS1700.850.1 has a significantly higher L'_{CO} than any of the 35 unlensed SMGs in the Bothwell et al. (2013) survey. Comparably ^{12}CO-luminous SMGs were found in a few cases – Ivison et al. (2013) identified a binary HyLIRG merger from a $\sim$200 deg^2 *Herschel* survey, while one lensed SMG from the $\sim$1300 deg^2 South Pole Telescope survey appears to be this luminous in ^{12}CO after a demagnification factor of $\sim 5\times$ (Hezaveh et al. 2013). Clearly finding SMGs with such high L'_{CO} has not been an easy task, even probing the widest field mm-wave surveys.

HS1700.850.1 is somewhat under-luminous in ^{12}CO for its SFR (or a high efficiency star former) compared to the average relation from Tacconi et al. (2013) for *normal* star forming galaxies (shown in Fig. 5). However, compared to SMGs from Bothwell et al. (2013), HS1700.850.1 is not unusual in lying 2-3$\times$ above the relation, an observation that supports application of the ULIRG conversion rate from L'_{CO} to total molecular gas mass.

4.4 The environment of HS1700.850.1

Given the extreme nature of HS1700.850.1, we explore whether the surroundings of this SMG are unusually clustered. The environment of HS1700.850.1 is traced in great detail by the LBG survey in the field, presented in Fig. 6 as a histogram binned to 500 km s^{-1} to highlight any possible neighbouring galaxies. HS1700.850.1 appears to reside in a sparse region, with the closest (and only) neighbouring galaxy within $\pm$1500 km s^{-1} at z=2.807 and lying 5$'$ (2.5 Mpc) away. The LBG selection function appropriate to this field (see Steidel et al. 2014) suggests that only two LBGs are expected in a 1500 km s^{-1} region from the 243 spectroscopic LBGs with measured redshifts in this field, thus finding only one about HS1700.850.1 is not statistically significant. There is one modest over density of six sources at $z = 2.751$, which includes the QSO HS1700+64 itself, contrasting with the sparse HS1700.850.1 environment nearby. Off the figure, at $z = 2.31$, there is a large over-density consistent with a forming proto-cluster (Steidel et al. 2005).

Using the extensive spectroscopic database of the KBSS survey, Trainor & Steidel (2012) study similar extreme sources to HS1700.850.1 at z=2.5-3.5 – HyLIRG quasars (HLQSOs). They find the HLQSOs themselves are associated with a $\delta\sim$7 overdensity in redshift when considered on scales of $\sim$5 h^{-1} Mpc, corresponding to a velocity scale of $\sigma_{v,pec}$ = 200 km s^{-1} and a projected scale of R$\sim$200 proper kpc. By studying the redshifts of galaxies around each HLQSO, they find however that there are no overdense peaks of similar significance. Repeating this procedure on random galaxy redshifts shows that the HLQSOs are correlated with much more significant small-scale overdensities than the average galaxy. They deduce that each HLQSO in their sample inhabits a DM halo with mass $\log(M_h/M_\odot) > 12.1\pm0.5$, or a median halo mass of $\log(M_{h,med}/M_\odot) = 12.3\pm0.5$. Crucially, the number density of these halos exceeds the number density of HLQSOs by a factor $\sim 10^6 - 10^7$, prompting the conclusion that the host halos of HLQSOs are not rare. Clearly HS1700.850.1 follows this trend, inhabiting an environment that is indistinguishable from the average field galaxy density in Fig. 6.

The scarcity of HLQSOs is likely due to an extremely improbable small-scale phenomenon that produces HLQSOs, possibly related to an atypical galaxy interaction geometry or similar scenario, or else extremely short durations of the events. Analogously in HS1700.850.1 and other extreme SMGs, an unlikely merger trajectory perhaps with unusually gas-rich progenitors (e.g., Narayanan et al. 2010) may explain rare bursts approaching $S_{850\mu m}$ $\sim$20 mJy and L_{IR} $\sim$ 2×10^{13} $L_\odot$ (e.g., Ivison et al. 2013). This motivates obtaining more detailed followup of the resolved double-peaked ^{12}CO emission in HS1700.850.1 to better understand the circumstances generating such enormous star formation rates and illuminated dust masses. We might also hypothesize that a very short duration starburst could explain the extreme luminosity of HS1700.850.1. For example, if we assumed that every $S_{850\mu m}$=15-20 mJy SMG was a brief episode in the more numerous 5 mJy SMG population (1000$\times$ more numerous in the ALMA-based counts of Simpson et al. 2015b, but still very luminous starbursts in themselves), then the HyLIRG burst would last only 50 kyr of a characteristic burst of 50 Myr (e.g., Chapman et al. 2005, Tacconi et al. 2006). This may not be a well motivated scenario – such a short timescale could likely only be driven by intense, hot AGN activity, yet there is no sign of an AGN in HS1700.850.1. Further, an AGN could not boost the 850μm emission while keeping the typical SMG appearance in Fig. 4. Most likely the SMG HyLIRGs are driven by a combination of factors.

Another estimate on the halo mass can be obtained using dynamical mass estimates from the peculiar velocities and the projected scale of the galaxy overdensities. With this approach Trainor & Steidel (2012) estimate HLQSOs are on average associated with even larger group-sized environments with total mass $\log(M_{grp}/M_\odot)\sim$13. The SMG clustering analysis in Hickox et al. (2012) suggested that the SMG population is hosted by haloes of comparable mass (see also Blain et al. 2004). This overdense environment with small relative velocities would increase the probability of a rare event, but an unusual merger configuration is still likely required to generate such large luminosities. In HS1700.850.1, even a group environment of this mass is unlikely based on the lack of explicit companions within 1500 km s^{-1} and within $\sim$2.5

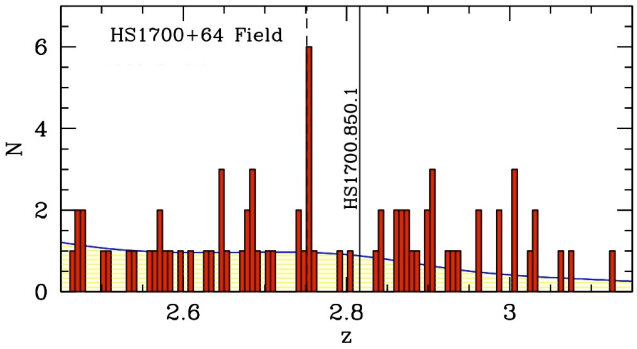


Figure 6. The environment of HS1700.850.1 derived from the LBG survey in the field, with 500 km s^{-1} bins to highlight any possible neighbouring galaxies (the closest one at z=2.807 lies 5$'$ away). HS1700.850.1 appears to reside in a relative void, although the selection function suggests only two expected LBGs in a 1500 km s^{-1} region for the 243 spectroscopic galaxies from z = 1.5–3.5 measured in this field (the overall redshift selection function for the continuum-selected redshift survey in all 15 fields of KBSS is shown as a blue line – see e.g. Steidel et al 2014). There is a 6-object galaxy spike at the redshift of the QSO HS1700+64 itself, contrasting the sparse environment of HS1700.850.1, while at $z = 2.31$ (off the plot axes) there is in fact a very large galaxy over-density consistent with a forming proto-cluster (Steidel et al. 2005).

Mpc. However, a $\sim 10^{13}$ M$_\odot$ halo will typically only have a couple of bright LBG-class galaxies in it, and might be easy to miss in an incomplete spectroscopic survey.

The Trainor & Steidel (2012) analysis has clearly demonstrated that HyLIRG-class sources do not require environments very different from their much less luminous counterparts. Evidently, the exceedingly low space density of at least HLQSOs ($\sim 10^{-9}$ Mpc^{-3}) results from a one-in-a-million event on scales $\ll 1$ Mpc, and not from being hosted by rare dark matter halos. HS1700.850.1 appears to inhabit a similarly typical halo. A moderate mass environment was also noted for a highly significant association of 8 SMGs at $z\sim$1.99 by Chapman et al. (2009), whilst revealing that z=2–3.5 SMGs generally do not align well with LBG overdensities within the GOODS-N survey field. Similar anti-biasing of SMGs is noted in the ECDFS field (A. Danielson in preparation). Notable exceptions exist at higher redshifts, including a z=4.05 galaxy overdensity found through an association of bright SMGs (Daddi et al. 2009), the COSMOS z=5.1 structure (Capak et al. 2011), and HDF850.1, which apparently lies in a z=5.3 galaxy overdensity (Walter et al. 2012).

Miller et al. (2015) used the Hayward et al. (2013a) model for the SMG population to estimate typical environments of the brightest SMGs and associations of multiple SMGs found in $\sim$500 Mpc^3 volumes. This model is based on mock galaxy catalogues derived from the Bolshoi simulation (Klypin et al. 2011; Behroozi et al. 2013) and insights obtained from performing radiative transfer on hydrodynamical simulations (Hayward et al. 2011; Hayward et al. 2013b). Miller et al. (2015) find the SMGs inhabit a range of mass scales going down to the average cosmic density in the simulation, and rarely are found in the most massive regions at these $z = 2$–3 epochs (although at significantly higher redshifts they are better tracers of the most massive regions). The surrounding LBG survey indeed suggests HS1700.850.1 is statistically consistent with inhabiting the average cosmic density.

5 CONCLUSIONS

We presented an IRAM-PdBI spectral survey of the HyLIRG HS1700.850.1, the brightest 850μm source found in the SCUBA-2 survey of the HS1700+64 field, and indeed all six SCUBA-2/KBSS fields. Our primary goal was to identify its redshift, guided by photometric redshift estimates in the optical through far-IR, and study its properties and environment. We conclude:

• The redshift for HS1700.850.1 is z=2.816, secured through the ^{12}CO(3–2) and (5–4) lines, validating the use of crude photometric redshifts to guide ^{12}CO redshift searches.

• The clear doubled-peaked profile of HS1700.850.1 in both CO transitions is likely a result of an end stage merger, within 6 kpc, as constrained by the size of the 850μm emission.

• HS1700.850.1 exhibits typical L$'_{\rm CO}$ for its far-IR luminosity or SFR compared to other unlensed SMGs, although its L$'_{\rm CO}$ is significantly larger than any SMGs identified in the Bothwell et al. (2013) survey.

• The environment of HS1700.850.1 is indistinguishable from the average field galaxy density, and no nearby LBG companions are identified within 1500 km s^{-1}. The HyLIRG burst could result from a 10^{-6} unlikely event on scales $\ll 1$ Mpc, and not from being hosted by a rare dark matter halo, but could also be due to a very short ~ 50 kyr burst timescale.

ACKNOWLEDGMENTS

We thank an anonymous referee for constructive comments on the manuscript. IRAM is supported by INSU/CNRS (France), MPG (Germany) and IGN (Spain). The Submillimeter Array is a joint project between the Smithsonian Astrophysical Observatory and the Academia Sinica Institute of Astronomy and Astrophysics and is funded by the Smithsonian Institution and the Academia Sinica. We thank summer students K. Lacaille and R. Perry for their work on the KBSS-SCUBA2 survey project. SCC acknowledges NSERC and CFI for support. FB acknowledges support through the Collaborative Research Centre 956, sub-project A1, funded by the Deutsche Forschungsgemeinschaft (DFG). IRS acknowledges support from STFC, a Leverhulme Fellowship, the ERC Advanced Investigator programme DUSTYGAL 321334 and a Royal Society/Wolfson Merit Award. JEG acknowledges support from the Royal Society.

REFERENCES

Behroozi P. S., Wechsler R. H., Conroy C., 2013a, ApJ, 770, 57
Bertoldi F., et al. 2007, ApJS, 172, 132
Blain, A., Chapman, S., Smail, I., Ivison R., 2004, ApJ, 611, 725
Boriello, A., Salucci, P., & Danese, L. 2003, MNRAS, 341, 1109
Borys, C.,Chapman, S; Halpern, M; Scott, D. 2003, MNRAS, 344, 385
Bothwell M., et al., 2013, MNRAS, 205, 1511
Capak et al. 2011, Nature, 470, 233
Chabrier G., 2003, PASP, 115, 763
Chapman S., Blain A., Smail I., Ivison R. 2003, Nature, 422, 695
Chapman S., Blain A., Smail I., Ivison R. 2005, ApJ, 622, 772
Chapman S., Blain A., Ibata R., Ivison R., Smail I., Morrison G. 2009, ApJ, 691, 560
Chapman S., et al. 2015, MNRAS, 449L, 68
Cole, S., et al. 2001, MNRAS, 326, 255
Combes, F. 2002, New Astronomy Reviews, 46, 755
Coppin, K., et al., 2006, MNRAS, 372, 1621
Daddi E., et al., 2009, ApJ, 673, L21
Digby-North, et al., 2010 MNRAS, 407, 846
Downes, D. & Solomon, P. M. 1998, ApJ, 507, 615
Elmegreen, B. G. 1999, ApJ, 517, 103
Fu, H., et al., 2013, Nature, 498, 338
Geach, J., et al., 2013, MNRAS, 432, 53
Greve, T. R., Ivison, R. J., Bertoldi, F., Stevens, J. A., Dunlop, J. S., Lutz, D., Carilli, C. L., 2004, MNRAS, 354, 779
Harris, A. I., et al. 2012, ApJ, 752, 152
Hayward C. C., Jonsson P., Keres D., Magnelli B., Hernquist L., Cox T. J., 2012, MNRAS, 424, 951
Hayward C. C., Keres D., Jonsson P., Narayanan D., Cox T. J., Hernquist L., 2011, ApJ, 743, 159
Hayward C. C., Narayanan D., Keres D., Jonsson P., Hopkins P. F., Cox T. J., Hernquist L., 2013b, MNRAS, 428, 2529
Hezaveh, Y. et al. 2013, ApJ, 767, 132
Hickox et al. 2012, MNRAS, 421, 284
Ivison R., et al., 2013, MNRAS, 412, 1913
Ivison R., et al., 2010, MNRAS, 404, 198
Ivison, R., et al., 1998, MNRAS, 298, 583
Karim, A., et al., 2013, MNRAS, 432, 2
Keeton, C. R. 2001, ApJ, 561, 46
Kennicutt, R. C., Jr. 1983, ApJ, 272, 54
Li, A. & Draine, B. T. 2001, ApJ, 554, 778
Loewenstein, M. & Mushotzky, R. F. 2003, NuPhS, 124, 91

Miller, T., Hayward, C., Chapman S., Berhoozi P., 2015, MNRAS, in press
Mocanu, et al., 2013, ApJ, 779, 61
Murray, N., Quataert, E., & Thompson, T. A. 2005, ApJ, 618, 569
Narayanan, D., Hayward, C. C., Cox, T. J., Hernquist, L., Jonsson, P., Younger, J. D., Groves, B., 2010, MNRAS, 401, 1613
Netzer, N., Elitzer, M., 1993, ApJ, 410, 701
Oliver, S., et al., 2010, A&A, 518L, 21
Planck collaboration et al. 2014, A&A, 571, 28
Pope, A., et al. 2006, MNRAS, 370, 1185
Rudie, G., et al., 2012, ApJ, 750, 67
Scott, K., et al. 2008, MNRAS, 385, 2225
Shapley, A., et al., 2005, ApJ, 626, 698
Simpson, J., et al., 2014, ApJ, 788, 125
Simpson, J., et al., 2015a, ApJ, 799, 81
Simpson, J., et al., 2015b, submitted
Smail, I., Ivison, R. J., Blain, A. W., & Kneib, J.-P. 2002, MNRAS, 331, 495
Steidel, C. C., et al. 2014, ApJ, 795, 165
Steidel, C., et al 2011, ApJ, 736, 60
Steidel, C., Erb, D.K., Shapley, A.E., et al 2010, ApJ, 717, 289
Steidel, C., et al 2005, ApJ, 626, 44
Steidel, C., Adelberger, K., Shapley, A., et al. 2000, ApJ, 532, 170
Swinbank, A.M., et al., 2010, Nature, 464, 733
Swinbank, M., et al. 2014, MNRAS, 438, 1267
Tacconi L. J. et al., 2013, ApJ, 768, 74
Tacconi L. J., Neri, R., Chapman, S., 2006, ApJ, 640, 228
Trainor and Steidel, C., 2012, ApJ, 752, 39
Vieira, J., et al., 2013, Nature, 495, 344
Walter, F., et al., 2012, Nature, 486, 233
Wardlow J., et al. 2011, MNRAS, 415, 1479
Weiss A., et a. 2009 ApJ 705, L45
Weiss A., Downes, D., Walter, F., Henkel, C.2005, A&A, 440L, 45
Younger, J., et al., 2008, ApJ, 688, 59
Younger, J., et al., 2010, MNRAS, 407, 1268
Zavala et al., 2015, MNRAS, accepted, aph150604747